

## Supporting Information

for *Adv. Funct. Mater.*, DOI: 10.1002/adfm.202205330

**K<sup>+</sup> Induced Phase Transformation of Layered Titanium Disulfide Boosts Ultrafast Potassium-Ion Storage**

*Xiao Zhang, Hezhen Zhu, Qiu He, Ting Xiong, Xuanpeng Wang,\* Zhitong Xiao, Hong Wang, Yan Zhao, Lin Xu, and Liqiang Mai\**

## Supporting Information

K<sup>+</sup> Induced Phase Transformation of Layered Titanium Disulfide Boosts Ultra-fast Potassium-Ion Storage

Xiao Zhang,<sup>#</sup> Hezhen Zhu,<sup>#</sup> Qiu He,<sup>#</sup> Ting Xiong, Xuanpeng Wang,<sup>\*</sup> Zhitong Xiao, Hong Wang, Yan Zhao, Lin Xu, and Liqiang Mai<sup>\*</sup>

### Experimental Section

#### Materials characterization

TiS<sub>2</sub> powder was purchased from Nanjing MKNANO Tech. Co., Ltd.. MCMB powder was purchased from SZKEJING. The crystal structure of TiS<sub>2</sub> was characterized via XRD (D-MAX/2000-PC, Rigaku), and HRTEM (HR-TEM, JEM-ARM200F/JEOL, operating at 200 kV) combined with EDX (system attached to the HR-TEM instrument). Morphology was analyzed by SEM (JSM-6500, JEOL, acceleration voltage: 20 kV).

#### Electrochemical characterization

The working electrode was prepared by casting slurry containing TiS<sub>2</sub> (70 wt%), acetylene black (20 wt%), and PVDF binder (10 wt%) of onto aluminum (Al) foil. The loading content of the anode materials on Al foil was about 1.0 mg cm<sup>-2</sup>. K metal was used as the counter electrode for half cells. The glass fiber (GF/D) was elected as separator. 1.0 M solution consist of KPF<sub>6</sub> in a 4/3/2 (v/v/v) mixture of ethylene carbonate (EC), dimethyl carbonate (DMC), and ethyl methyl carbonate (EMC) was used as the electrolyte. The full-cells were assembled with MCMB cathode and TiS<sub>2</sub> anode. To prepare the cathodes, MCMB, acetylene black, and PVDF binder were mixed with a weight ratio of 8:1:1. For the full cells, the mass ratio of MCMB cathode to TiS<sub>2</sub> anode was fixed at 4:1. The CV test was carried out using a ZIVE-MP2A. The galvanostatic discharge/charge test was conducted on LAND CT2001A. The GITT data were collected by applying a current of 20 mA g<sup>-1</sup> for 3 minutes, followed by 1 hour of rest.

#### Calculation method

Materials Studio 2020 CASTAP module was used for density functional theory calculations.<sup>[1]</sup> The intercalation energy of K<sup>+</sup> at different concentration (K<sub>n</sub>TiS<sub>2</sub>, n = 0.125, 0.25, 0.375, 0.5, 0.625, 0.75, 0.875) and corresponding variation of layer spacing were evaluated. In addition, some electronic structures and the migration path of K between the interlayers of TiS<sub>2</sub> were also simulated.<sup>[2]</sup> The generalized gradient approximation (GGA) and the Perdew–Burke–Ernzerhof (PBE) exchange–correlation function were used.<sup>[3]</sup> The calculations were performed with fine quality, and the dispersion force was corrected by

Grimme method.<sup>[4]</sup> In detail, the electronic self-consistent field (SCF) tolerance was  $1 \times 10^{-6}$  eV/atom, while the force tolerance in geometry optimization was 0.03 eV/Å, and the plane wave basis energy cutoff was set as 435.4 eV. The insertion energies were calculated with a supercell,  $K_nTi_8S_{16}$  ( $n=1, 2, 3, 4, 5, 6, 7$ ), and the insertion energy and average insertion energy were calculated by following equations, respectively.

$$E = E(K_nTi_8S_{16}) - E(K_{n-1}Ti_8S_{16}) - E(K)$$
$$E_{avg} = \frac{E(K_nTi_8S_{16}) - E(Ti_8S_{16})}{n}$$

In above equations,  $E(x)$  represents the energy of the structure,  $x$ , and  $E(K)$  is the normalized energy of bulk K metal.

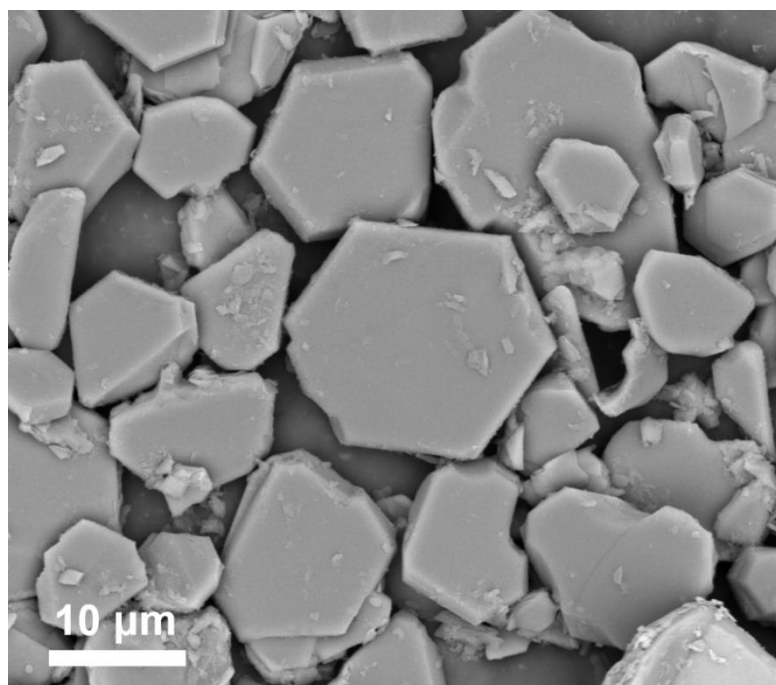


**Figure S1.** SEM image of  $TiS_2$ .

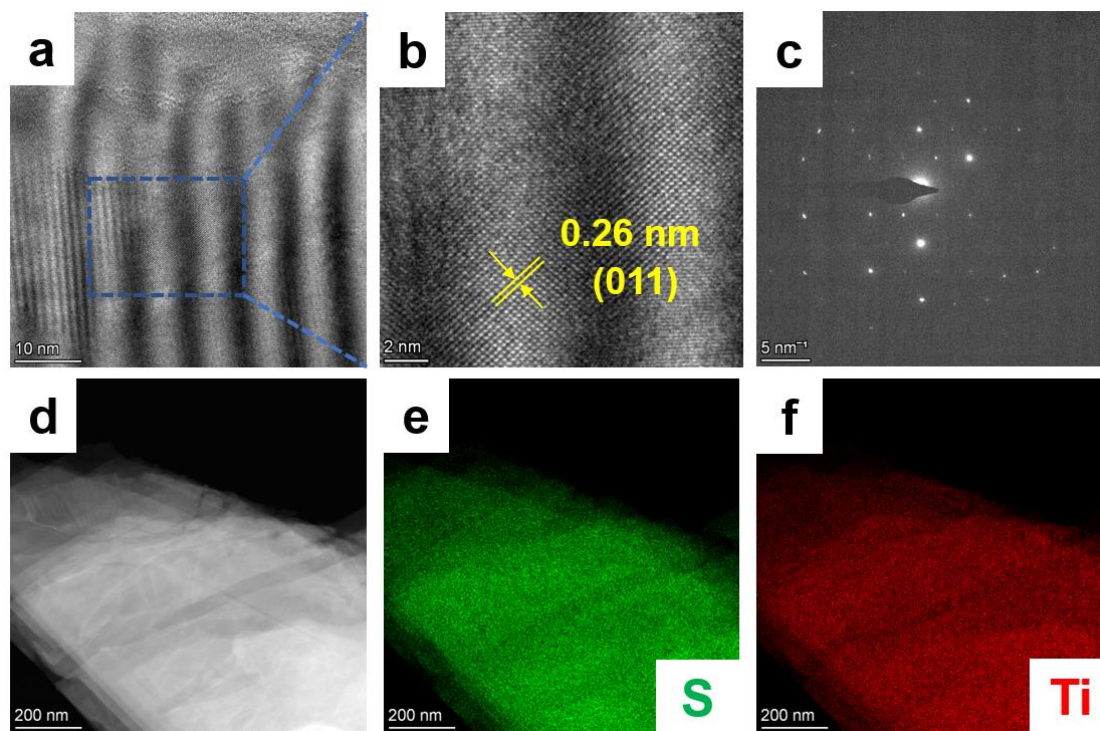


**Figure S2.** (a-b) HRTEM image and (c) the corresponding SAED pattern of  $\text{TiS}_2$ . (d-f) The corresponding elemental mapping images of S and Ti.

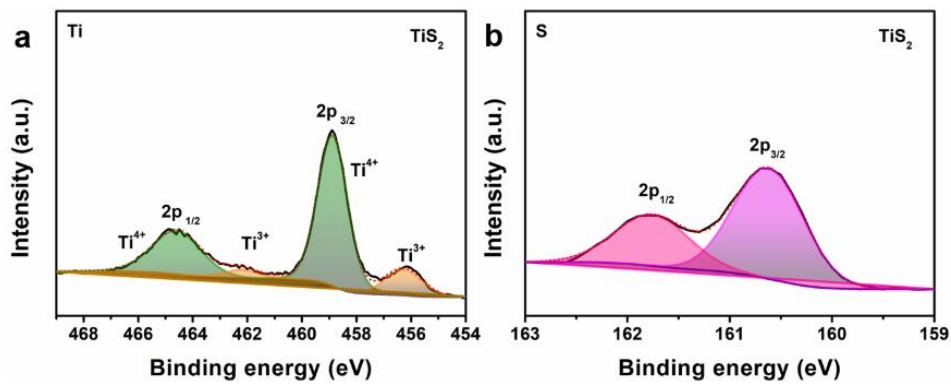


**Figure S3.** XPS spectra (a) Ti 2p and (b) S 2p of  $\text{TiS}_2$ .

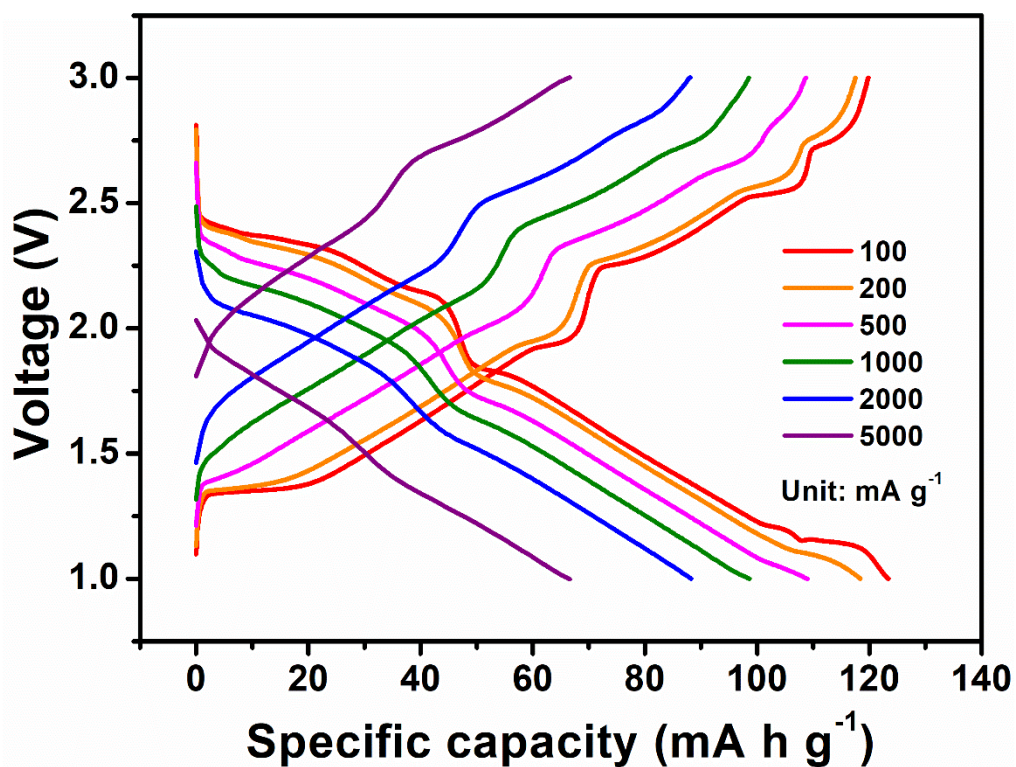


Figure S4. GCD curves of TiS<sub>2</sub> anode in half cells at different current densities.

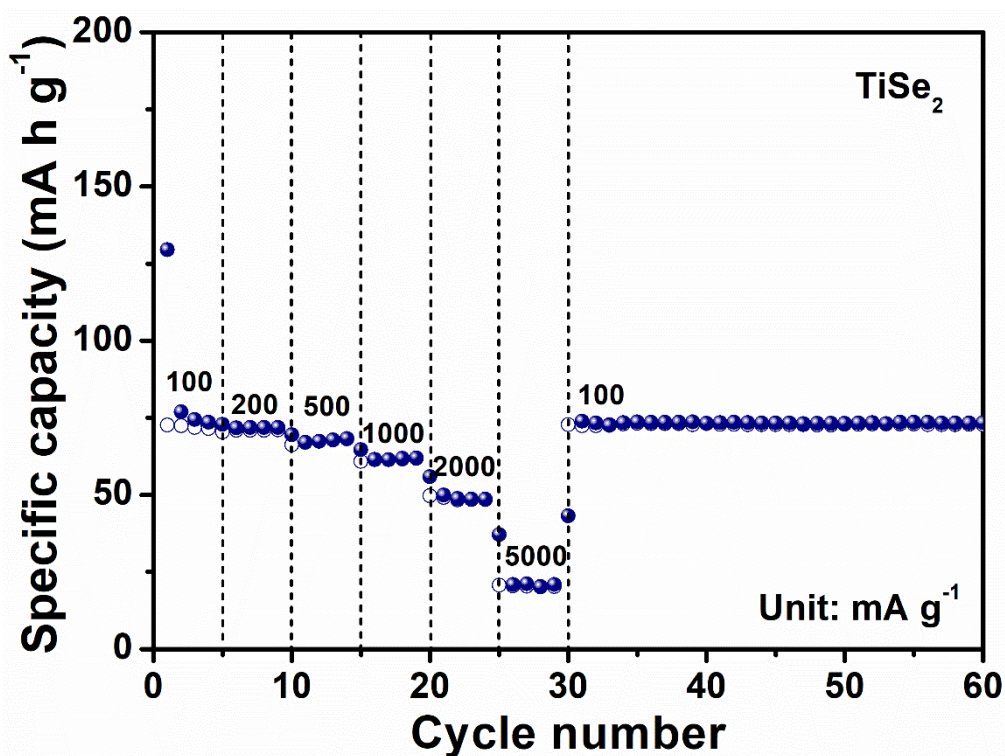


Figure S5. Rate capability of TiSe<sub>2</sub> anode.

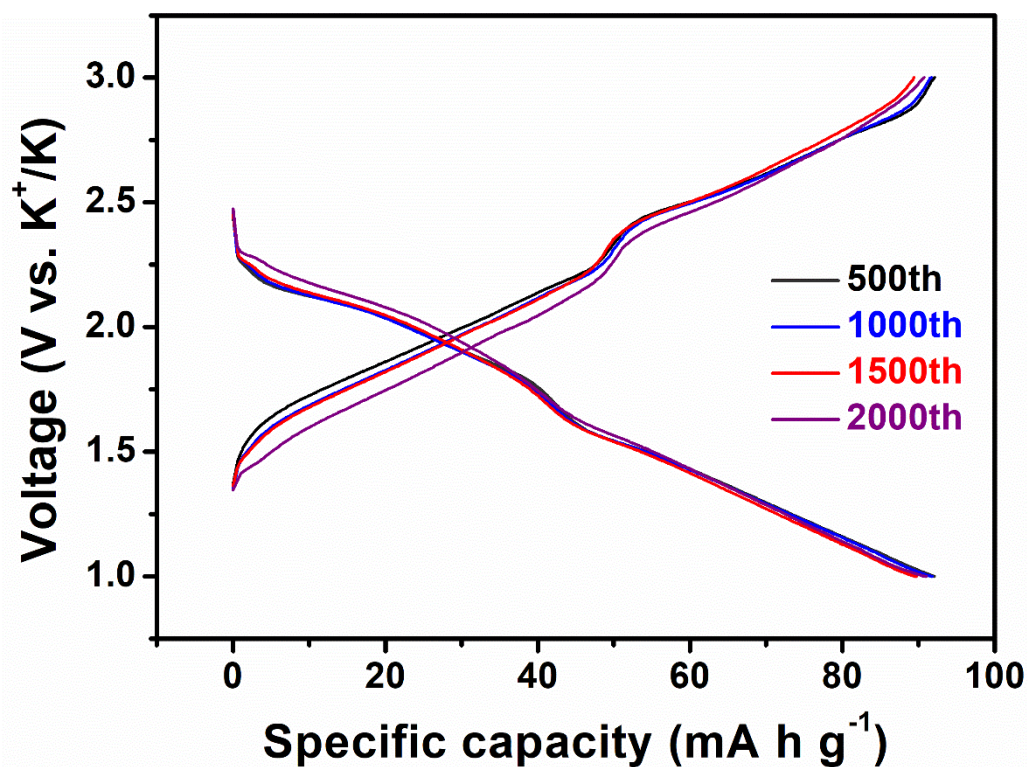


Figure S6. GCD Profiles of the  $\text{TiS}_2\text{-K}$  battery at different cycles at  $1000 \text{ mA g}^{-1}$ .

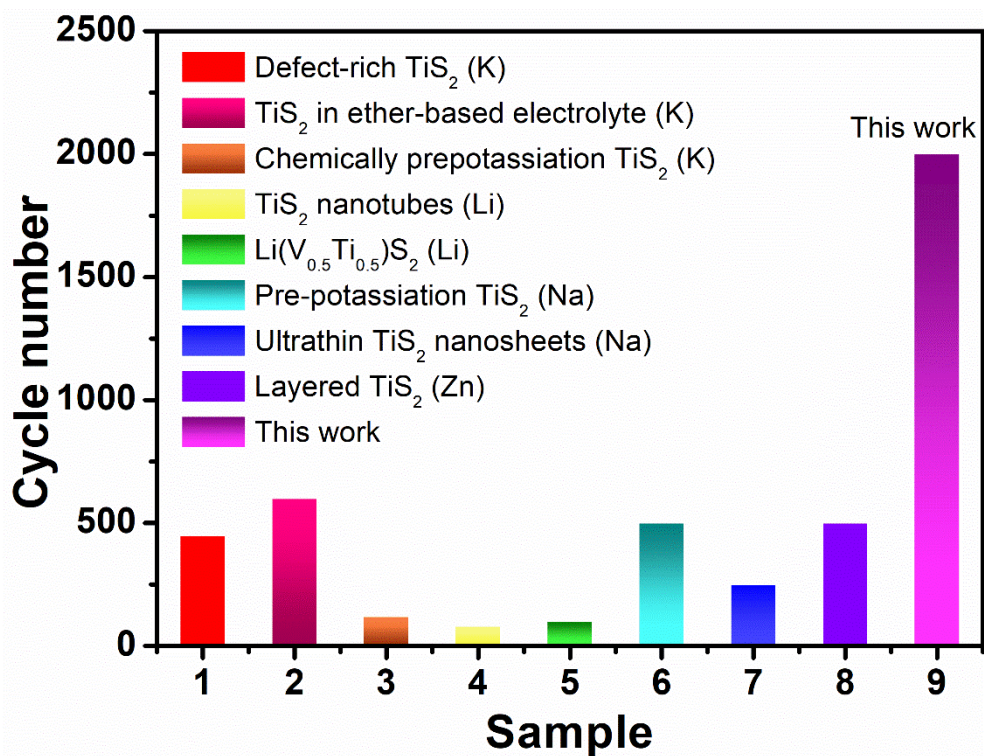
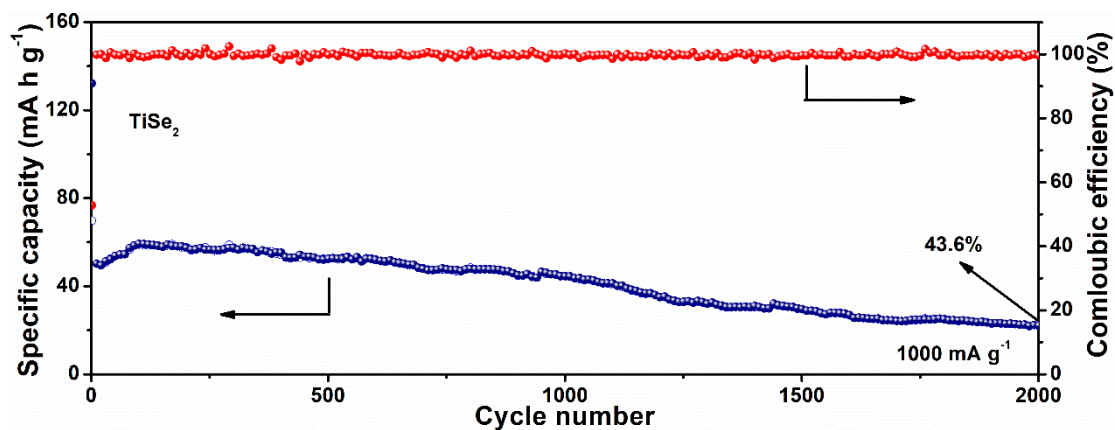
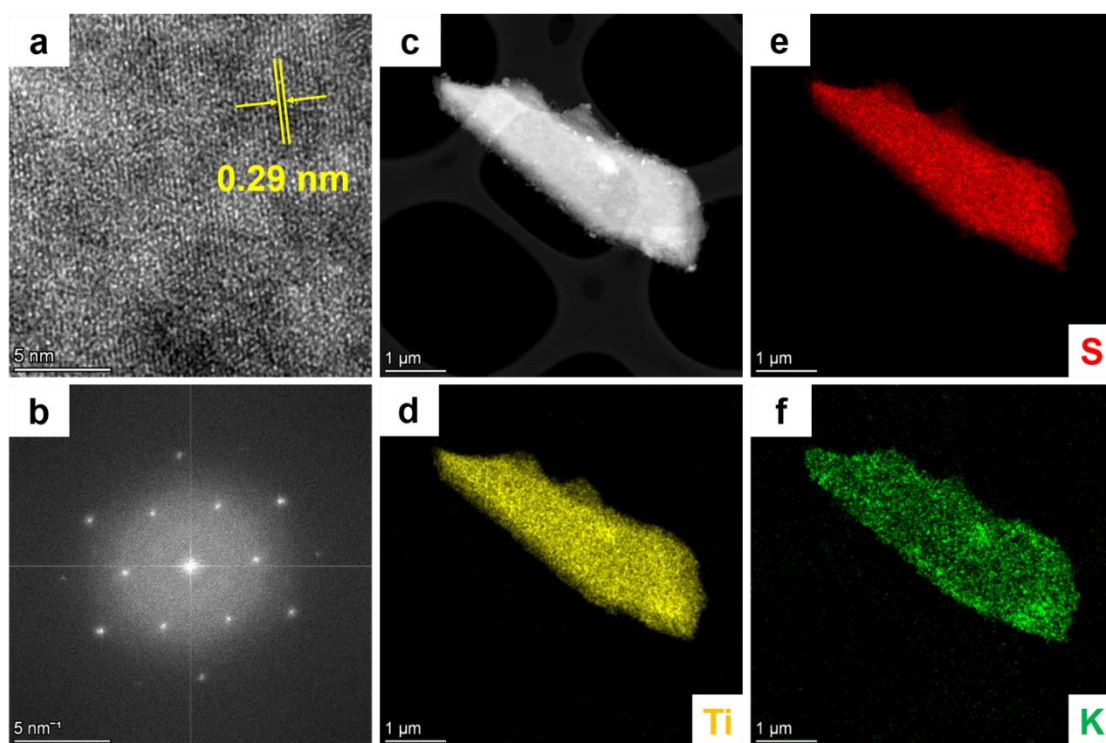


Figure S7. Cycle performance comparison with previous literature.



**Figure S8.** Long-term cycle performance at  $1000 \text{ mA g}^{-1}$  of  $\text{TiSe}_2$  anode.



**Figure S9.** (a) HRTEM image and (b) the corresponding SAED pattern of  $\text{TiS}_2$  at potassiation state. (c-f) The corresponding elemental mapping images of Ti, S, and K.

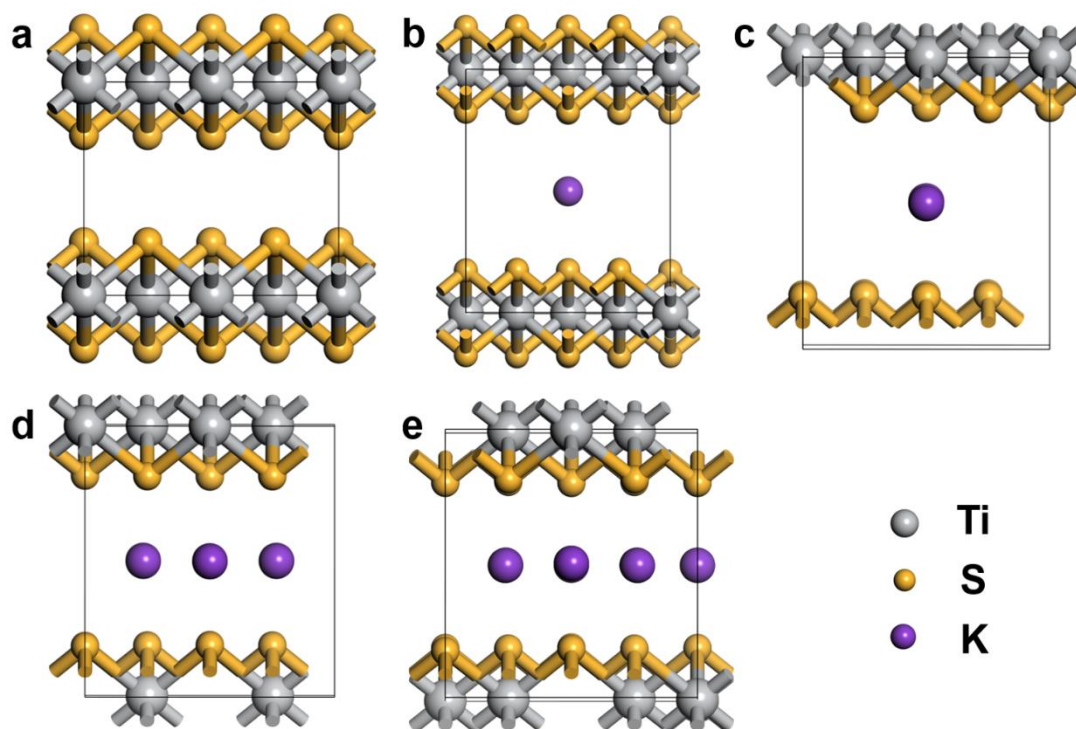


**Figure S10.** The crystal structure of (a) TiS<sub>2</sub>, (b) K<sub>0.125</sub>TiS<sub>2</sub>, (c) K<sub>0.25</sub>TiS<sub>2</sub>, (d) K<sub>0.75</sub>TiS<sub>2</sub>, and (e) K<sub>0.875</sub>TiS<sub>2</sub>.

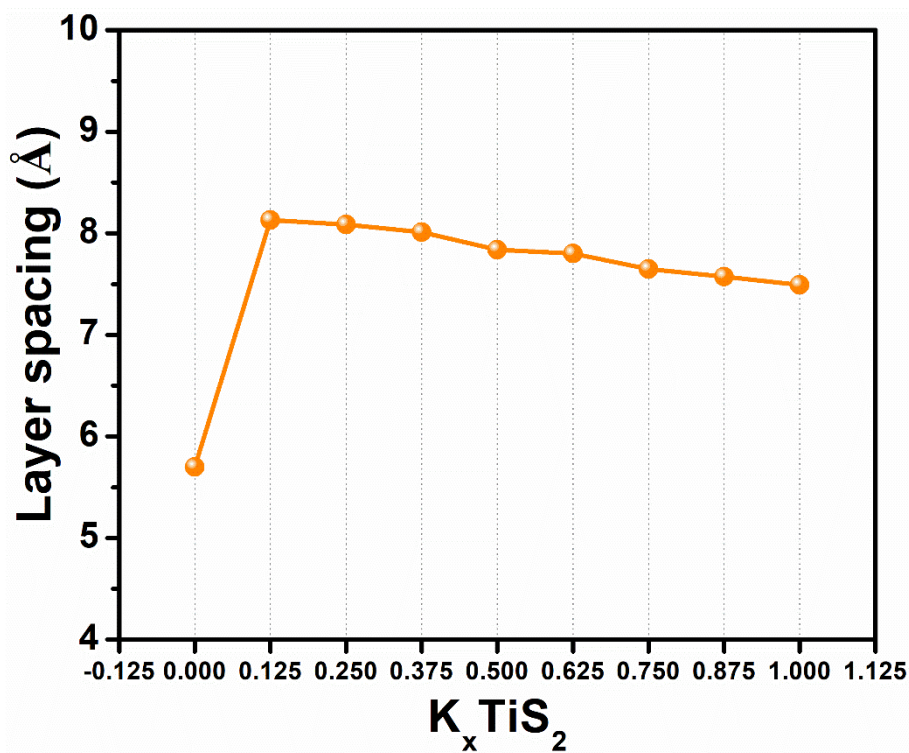


**Figure S11.** The calculated layer spacing variation function of K content.



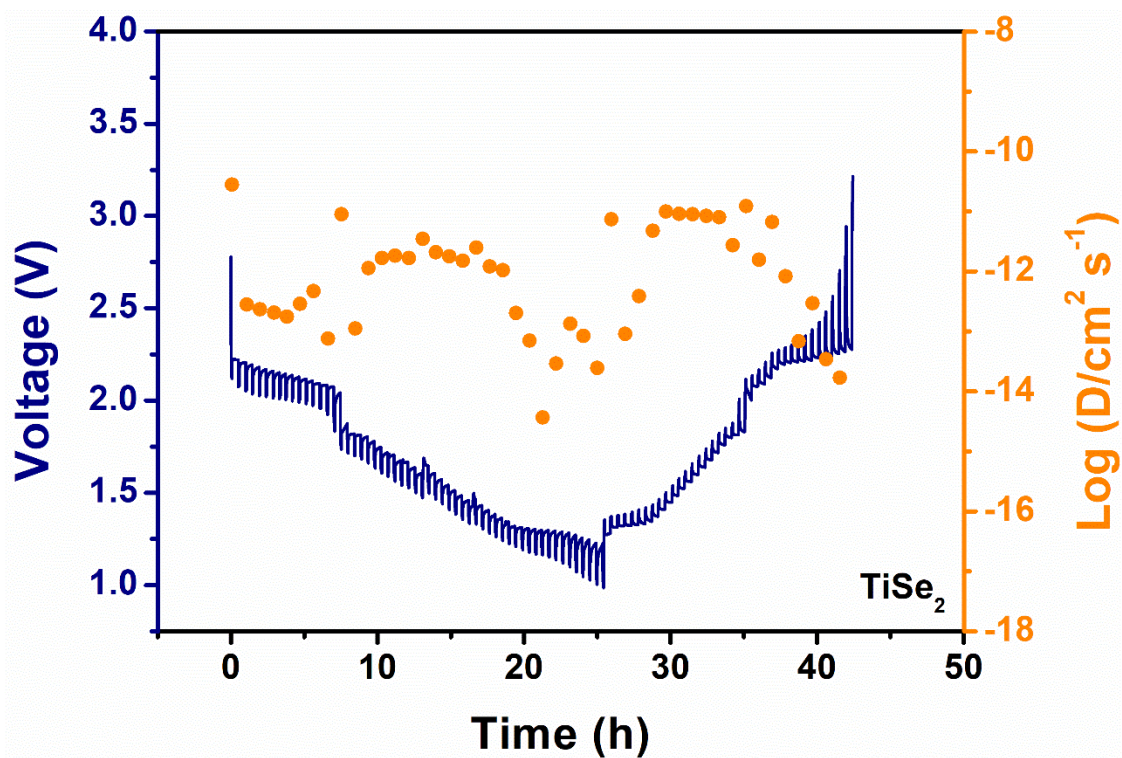


Figure S12. GITT voltage profiles and diffusion coefficients versus state of charge and discharge of  $\text{TiSe}_2$  anode.

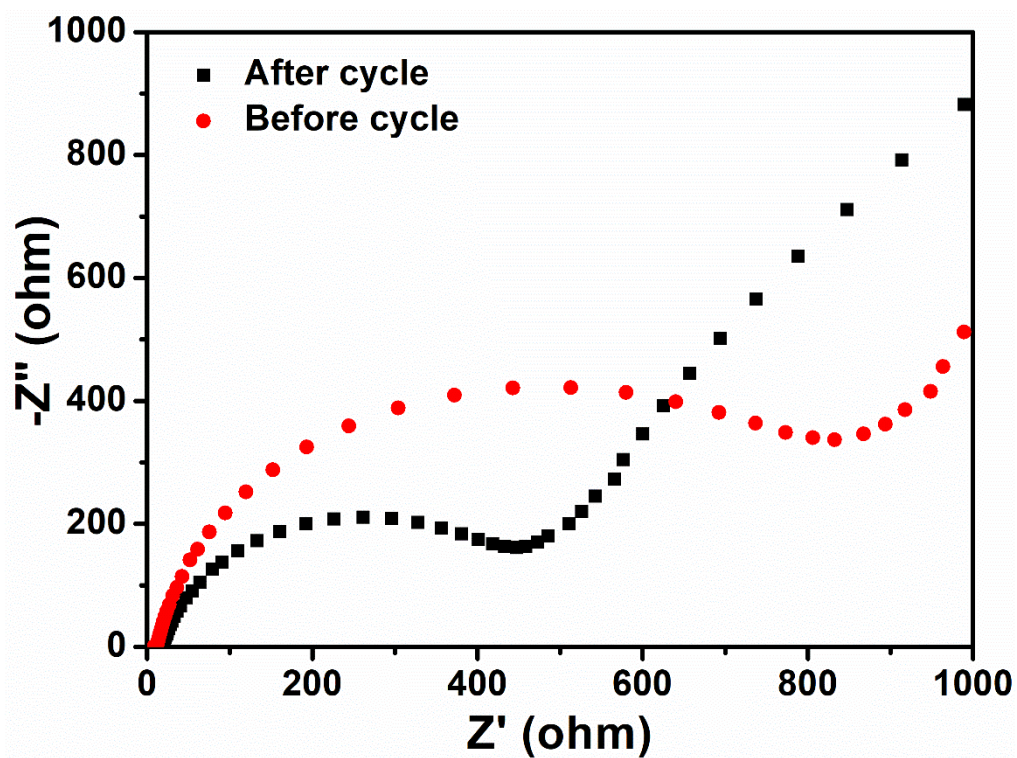
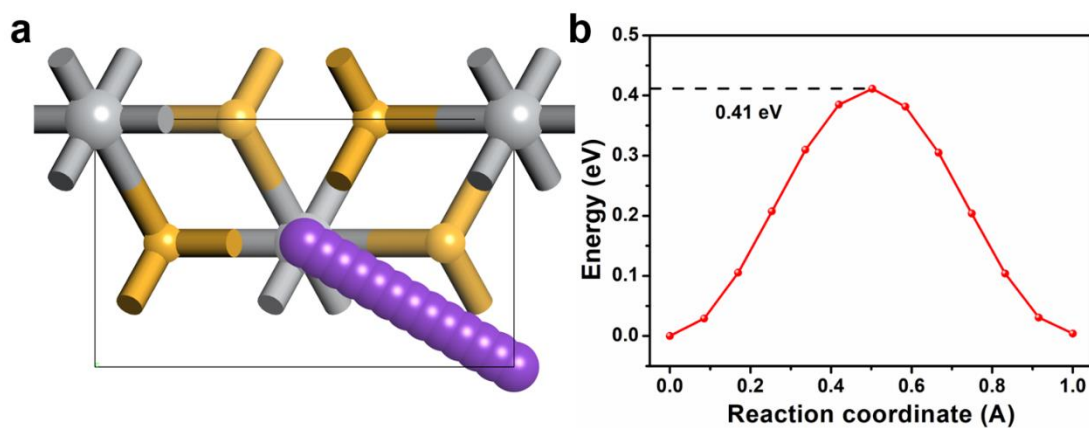
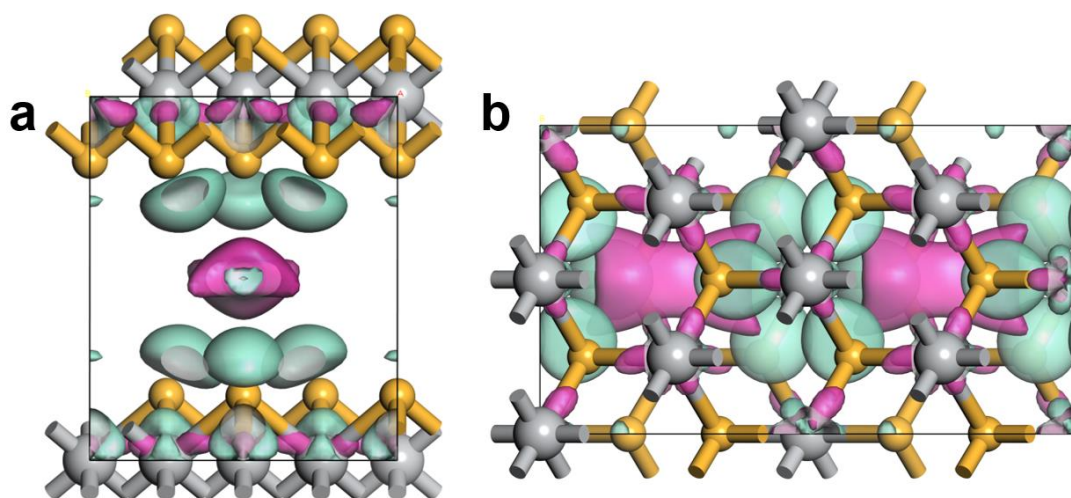


Figure S13. Nyquist plots of  $\text{TiS}_2$  before and after cycling.



**Figure S14.** The proposed  $K^+$  (a) diffusion path and (b) energy barriers in  $K_{0.5}TiS_2$ .



**Figure S15.** The local charge density difference isosurface.

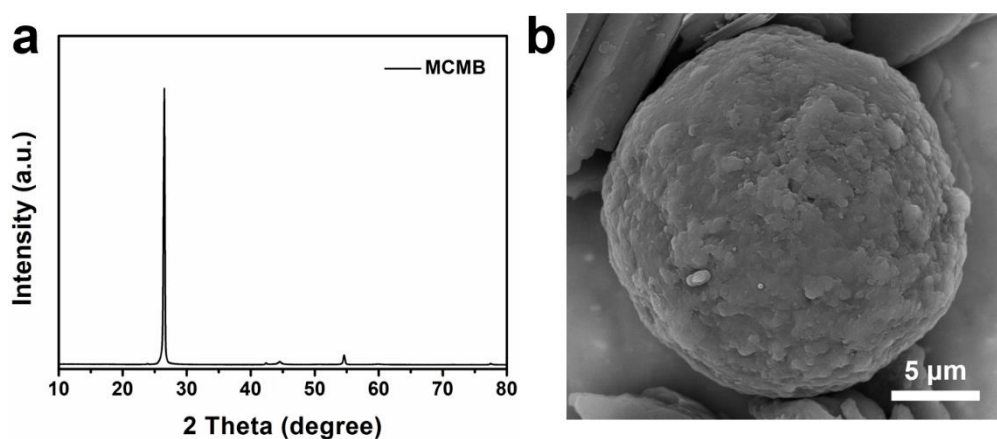


**Figure S16.** (a) The XRD pattern and (b) SEM image of MCMB powder.

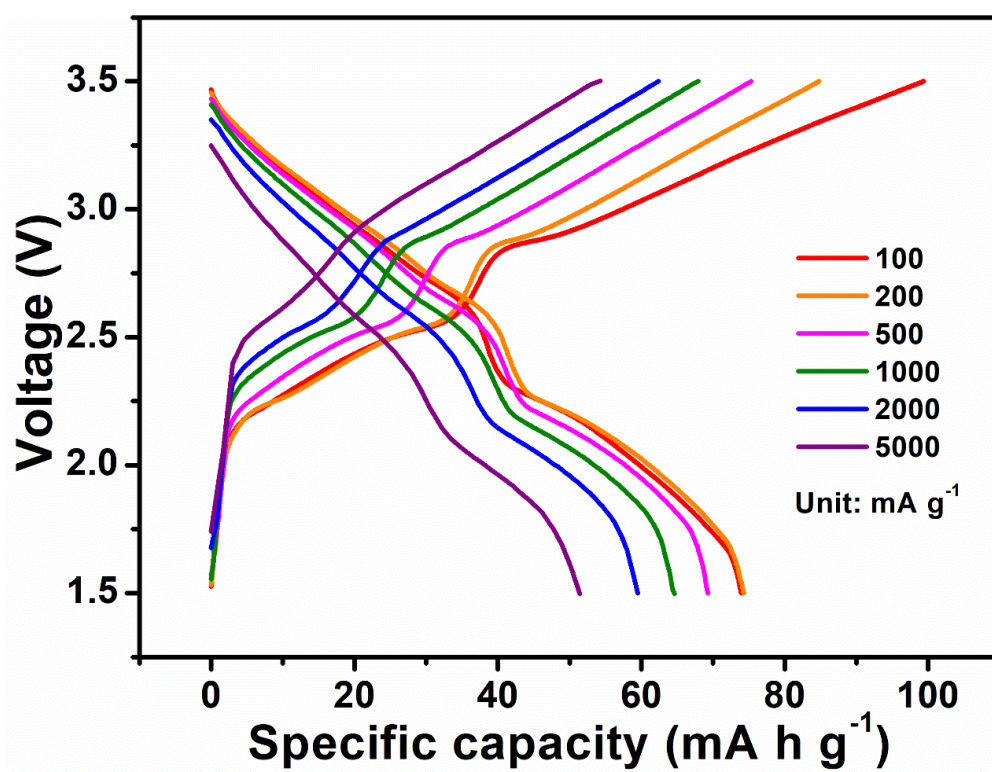


Figure S17. The GCD curves of TiS<sub>2</sub> anode in full cells at different current densities.

Table S1. Diffusion barriers comparison with previous literature.

<b>Materials</b>	<b>Diffusion barriers (eV)</b>	<b>Ref.</b>
Defect-rich TiS <sub>2</sub>	2.446	[5]
VS <sub>2</sub> nanosheets	0.51	[6]
CoV <sub>2</sub> O <sub>6</sub> nanosphere@graphene oxide (GO)	0.5	[7]
Sn	0.6	[8]
Dipotassium terephthalate (K <sub>2</sub> TP)	0.46	[9]
<b>K<sub>0.25</sub>TiS<sub>2</sub></b>	<b>0.27</b>	<b>This work</b>

## References

- [1] S. J. Clark, M. D. Segall, C. J. Pickard, P. J. Hasnip, M. I. J. Probert, K. Refson, M. C. Payne, *Z Krist-Cryst Mater.*, **2005**, 220, 567.
- [2] N. Govind, M. Petersen, G. Fitzgerald, D. King-Smith, J. Andzelm, *Comp. Mater. Sci.*, **2003**, 28, 250; P. J. Mohr, B. N. Taylor, D. B. Newell, *J. Phys. Chem. Ref. Data*, **2008**, 80, 633.
- [3] J. P. Perdew, K. Burke, M. Ernzerhof, *Phys. Rev. Lett.*, **1996**, 77, 3865.
- [4] S. Grimme, *J. Comput. Chem.*, **2006**, 27, 1787.
- [5] T. Liu, X. Zhang, M. Xia, H. Yu, N. Peng, C. Jiang, M. Shui, Y. Xie, T.-F. Yi, J. Shu, *Nano Energy*, **2020**, 67, 104295.
- [6] X. Zhang, Q. He, X. Xu, T. Xiong, Z. Xiao, J. Meng, X. Wang, L. Wu, J. Chen, L. Mai, *Adv. Energy Mater.*, **2020**, 10, 1904118.
- [7] H. Liang, Y. Zhang, S. Hao, L. Cao, Y. Li, Q. Li, D. Chen, X. Wang, X. Guo, H. Li, *Energy Storage Mater.*, **2021**, 40, 250.
- [8] J. Lang, J. Li, X. Ou, F. Zhang, K. Shin, Y. Tang, *ACS Appl. Mater. Interfaces*, **2019**, 12, 2424.
- [9] Y. Luo, L. Liu, K. Lei, J. Shi, G. Xu, F. Li, J. Chen, *Chem. Sci.*, **2019**, 10, 2048.